

© DIGITAL VISION

Toward Integrated Circuit Size Reduction

Hee-Ran Ahn and Bumman Kim

Because the scattering parameters are so closely associated with power transfer properties of a network, they permit the formulation of concise and useful expressions for the conservation of energy constraints in passive structures. They are, therefore, particularly suitable for the statement of network reliability requirements in the frequency domain and hence are useful in network synthesis problems. The earliest use of scattering parameters appears to be in the article written in 1920 [1], which deals with properties of ideal transformer networks simultaneously matched at all ports. Since that time, the scattering parameters have been studied [2], [3] and applied for various microwave passive components.

Hee-Ran Ahn (hrah@postech.ac.kr) and Bumman Kim (bmkim@postech.ac.kr) are with the Department of Electronic and Electrical Engineering, POSTECH (Pohang University of Science and Technology), Republic of Korea.

Digital Object Identifier 10.1109/MMM.2007.910937

If the passive components are terminated in arbitrary impedances (asymmetric passive components), any advantage to reduce total size of microwave integrated circuits can be expected.

However, since only the symmetric passive components have been developed, the theory has not been well known [4]. In this article, three different scattering matrices are introduced and compared, and a normalized scattering matrix is derived in a practical case of a two-port network terminated in arbitrary impedances. As one of its applications, design equations of impedance-transforming directional couplers are derived.

The first directional coupler was reported in 1922 [5] and significant progress was made during the 1940s and 1950s [6]–[7]. In the 1960s and 1970s, numerous papers [8]–[18] extended the theory, and their application and development have continued [19]. However, all the conventional theories and developments can be applied only for equal termination impedances even with asymmetric structures [9], [10], [18], [19]. Very recently, design equations of impedance-transforming directional couplers symmetrically terminated in arbitrary impedances were derived [20].

The study of asymmetric passive components first started with asymmetric ring hybrids in 1994 [21] and other asymmetric components including branch-line hybrids, three-port power dividers, phase shifters, attenuators, and impedance transformers were investigated during the last ten years [22]–[26]. If the passive components are terminated in arbitrary impedances (asymmetric passive components), any advantage to reduce total size of microwave integrated circuits can be expected. In this article, impedance-transforming directional couplers and their application to a feedforward amplifier are explained as an example of the advantages.

Impedance-Transforming Directional Couplers and Their Application to a Feedforward Amplifier

An impedance-transforming directional coupler and a feedforward amplifier [27], [28] are illustrated in Figure 1(a) and Figure 1(b), respectively. When a unity power is fed into port ① and its length of Θ is 90° in Figure 1(a), some part of the power is coupling into port ② and the remainder is transmitted to port ④. The coupling power is expressed as C^2 and its square root C is defined as a coupling coefficient. Theoretically, no power is delivered to port ③, which is called an isolation port. The feedforward amplifier shown in Figure 1(b) is used to reduce harmonics produced by a high-power amplifier and consists of a main amplifier, an error amplifier, and passive components; directional couplers (D1 and D2), delay lines (DL1 and DL2), and power combiners (PC1 and PC2). The feedforward amplifier has two cancellation loops, which are called a signal cancellation loop (the first loop) and an error cancellation loop (the second loop).

In the first loop in the feedforward amplifier in Figure 1(b), it is assumed an input signal $v_s(t)$ has two carrier frequencies f_1 and f_2 and that most of the input signal is fed into the main amplifier. The output signal of the main amplifier contains not only the amplified input signal but also harmonics h_1 and h_2 due to its nonlinear characteristics. Several types of harmonics are generated but only two located close to the carrier frequencies are considered because the two harmonics can not be removed easily. At point A in Figure 1(b), the remainder of the input signal is coupled into the delay line (DL1) and its output signal has only carrier frequencies. If it is assumed that the phase delay of the main amplifier is Θ_1 , the total phase delay at point B is $90^\circ + \Theta_1$ from the point A. If the phase difference between two points C and D is 180° and the output spectrum of the main amplifier is assumed to be directed upward as shown, then the output spectrum of the delay line (DL1) is directed downward. Therefore, the resulting output signal of the power combiner (PC1) has only harmonics and 90° out of phase with respect to the point C or D.

In the second loop in Figure 1(b), the error amplifier is a linear amplifier and thus its output signal contains

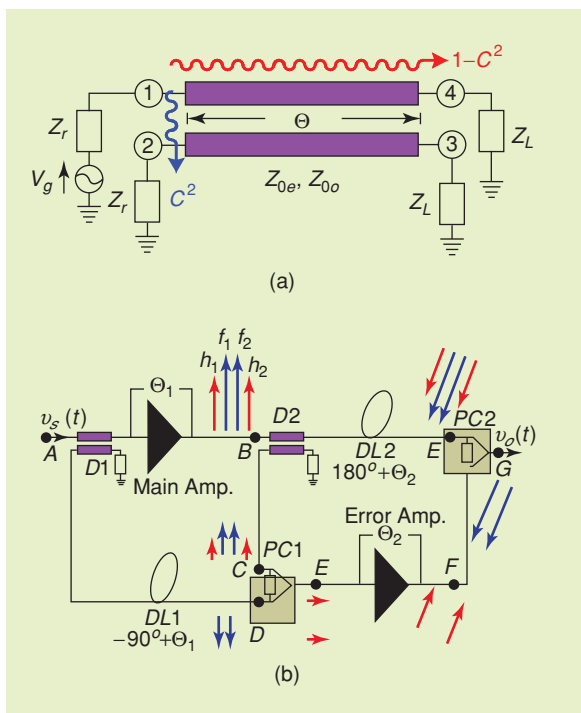


Figure 1. An impedance-transforming directional coupler and its application to a feedforward amplifier. (a) Directional coupler. (b) Feedforward amplifier.

only the harmonics. In a similar way, if the phase difference between two points E and F is 180° , the final output $v_o(t)$ contains only the amplified input signal without any harmonic.

In the feedforward amplifier in Figure 1(b), the input impedance of the main amplifier is generally complex and not equal to that at point A . Therefore, any matching process is needed for the best performance, and if the $D1$ directional coupler can transform a real impedance into another one, only a single stub is needed more for the imaginary part of the input impedance of the main amplifier. Similarly, when adding a single stub to the output stage of the main amplifier, its output impedance becomes a real impedance of a few ohms, which should be transformed into the final output stage at point G .

The delay lines are a kind of phase shifter and if they can be terminated in arbitrary impedances [26], the $DL1$ can transform the impedance at point A into that at point D . The power combiner $PC1$ also has an impedance transforming function [25] and transforms the impedance at point C or D into a real impedance of the input impedance of the error amplifier. In this way, no complex matching network is needed for the best performance of the feedforward amplifier.

If the termination impedances of the directional couplers, the delay lines, and the power combiners are fixed at 50Ω , additional input and output matching networks between the directional couplers, the main amplifier, the error amplifier, and the power combiners are needed and its resulting circuit becomes more complex.

Two-Port Scattering Parameters

To analyze the impedance-transforming directional couplers, a normalized scattering matrix, which was first introduced in 1965 [3], is needed. However, since only symmetric passive components have been developed during the last several decades, the theory has not been well known. The scattering matrices are classified in voltage-basis, current-basis, and normalized scattering parameters and dependent on termination impedances. The three different scattering matrices are the same in the case of equal termination impedances but only the normalized scattering matrix is correct in the case of arbitrary termination impedances. Therefore, normalized scattering matrix should be considered in the case of the impedance-transforming directional couplers.

Voltage- and Current-Basis Scattering Matrices

A two-port network with impedance or admittance parameters is illustrated in Figure 2 where $V_1^+, V_2^+, I_1^+, I_2^+$ are incident voltages and currents, $V_1^-, V_2^-, I_1^-, I_2^-$ are reflected ones, and the subscript number indicates each port. The incident waves are defined under the assumption that the two-port network is perfectly matched and the reflected waves are the difference between actual quantities and incident quantities. The

scattering matrix relating the ratio of the reflected voltage waves to the incident voltage waves is called the voltage-basis scattering matrix and expressed as

$$S_{pq}^V = \frac{V_p^-}{V_q^+} \Big|_{V_k^+ = 0 \text{ for } k \neq q}, \quad (1)$$

where p and q are the port number.

In other words, (1) explains that S_{pq}^V is found by driving port q with an incident wave of voltage V_q^+ , and measuring the reflected wave amplitude, V_p^- coming out of port p . The incident waves on all ports except the q port are set to zero, which means that all ports should be terminated in matched loads to avoid reflections. Thus, S_{pp}^V is the reflection coefficient seen looking into port p when all other ports are terminated in matched loads, and S_{pq}^V is the transmission coefficient from port q to port p , when all other ports are terminated in matched loads.

The scattering matrix relating the ratio of the reflected-current waves to the incident-current waves is called the current-basis scattering matrix and expressed as

$$S_{pq}^I = \frac{I_p^-}{I_q^+} \Big|_{I_k^+ = 0 \text{ for } k \neq q}. \quad (2)$$

In the case of a two-port network terminated in arbitrary impedances in Figure 2, the voltage-basis scattering parameters are written as

$$S_{11}^V = -\frac{[(Y_{11} - Y_r^*)(Y_{22} + Y_L) - Y_{12}Y_{21}]}{\Delta_y}, \quad (3a)$$

$$S_{12}^V = -\frac{1}{\Delta_y} Y_{12}(Y_L + Y_L^*), \quad (3b)$$

$$S_{21}^V = -\frac{1}{\Delta_y} Y_{21}(Y_r + Y_r^*), \quad (3c)$$

$$S_{22}^V = -\frac{[(Y_{11} + Y_r)(Y_{22} - Y_L^*) - Y_{12}Y_{21}]}{\Delta_y}, \quad (3d)$$

where $\Delta_y = (Y_{11} + Y_r)(Y_{22} + Y_L) + Y_{12}Y_{21}$, $Y_r = 1/Z_r$, $Y_L = 1/Z_L$ and Y_r^* and Y_L^* are complex conjugates of Y_r and Y_L .

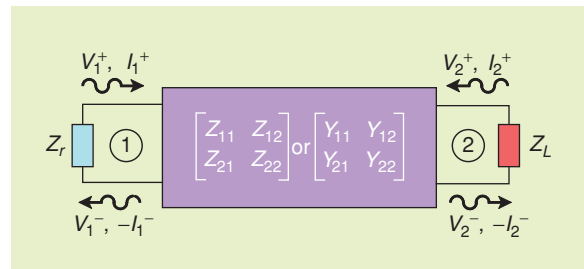


Figure 2. A two-port network with impedance or admittance parameters.

In a similar way, the current-basis scattering parameters are

$$S_{11}^I = \frac{[(Z_{11} - Z_r^*)(Z_{22} + Z_L) - Z_{12}Z_{21}]}{\Delta_z}, \quad (4a)$$

$$S_{12}^I = \frac{1}{\Delta_z} Z_{12}(Z_L + Z_L^*), \quad (4b)$$

$$S_{21}^I = \frac{1}{\Delta_z} Z_{21}(Z_r + Z_r^*), \quad (4c)$$

$$S_{22}^I = \frac{[(Z_{11} + Z_r)(Z_{22} - Z_L^*) - Z_{12}Z_{21}]}{\Delta_z}, \quad (4d)$$

where $\Delta_z = (Z_{11} + Z_r)(Z_{22} + Z_L) + Z_{12}Z_{21}$.

Normalized Scattering Matrix

The voltage- and current-basis scattering matrices exist for one two-port network and are correct only with the equal termination impedances. In the case of arbitrary termination impedances, a (complex) normalized scattering matrix is needed for the correct analyses and can be obtained from either current- or voltage-basis quantities. To introduce the normalization by which the normalized scattering matrix becomes basis independent, a definition of *paraconjugate Hermitian impedance and admittance matrices* r and g are first defined as

$$r = \frac{1}{2}(z + z^*) = h h^*, \quad (5a)$$

$$g = \frac{1}{2}(y + y^*) = k k^*, \quad (5b)$$

where $(z + z^*) = \begin{bmatrix} Z_r + Z_r^* & 0 \\ 0 & Z_L + Z_L^* \end{bmatrix}$ and

$$(y + y^*) = \begin{bmatrix} Y_r + Y_r^* & 0 \\ 0 & Y_L + Y_L^* \end{bmatrix},$$

and where z and y are reference impedance and admittance matrices in Figure 2. For the normalized scatter-

ing parameters, normalized incident-wave vector a and normalized reflected-wave vector b are defined as

$$a = h^* I^+ = k^* V^+ \quad (6a)$$

$$b = h I^- = k V^-. \quad (6b)$$

The equations in (6) mean that the normalized wave vectors are found under the assumption that the two-port network is terminated in square roots of the real impedances of the termination impedances. The normalized scattering matrix is defined to relate the incident and reflected waves as

$$b = S a. \quad (7)$$

The elements of S are called the (complex) normalized scattering parameters and can be expressed in terms of the impedance (admittance) matrix and the reference termination impedance (admittance) matrix as

$$S = h[Z + z]^{-1}[Z - z^*][h^*]^{-1} \quad (8a)$$

$$S = -k[Y + y]^{-1}[Y - y^*][k^*]^{-1}. \quad (8b)$$

In more detail for the case of the two-port network in Figure 2, the normalized scattering parameters and their relation to the voltage- basis and current-basis scattering parameters are written as

$$S_{11} = S_{11}^V = S_{11}^I, \quad (9a)$$

$$S_{12} = S_{12}^V \sqrt{\frac{\text{Re}(Y_r)}{\text{Re}(Y_L)}} = S_{12}^I \sqrt{\frac{\text{Re}(Z_r)}{\text{Re}(Z_L)}}, \quad (9b)$$

$$S_{21} = S_{21}^V \sqrt{\frac{\text{Re}(Y_L)}{\text{Re}(Y_r)}} = S_{21}^I \sqrt{\frac{\text{Re}(Z_L)}{\text{Re}(Z_r)}}, \quad (9c)$$

$$S_{22} = S_{22}^V = S_{22}^I. \quad (9d)$$

As shown in (9), the reflection scattering parameters are the same independently of the bases but transmission coefficients are dependent on the termination impedances (admittances). The formulas determining the normalized scattering parameters in (8) look simple but the calculations are sometimes quite complicated. For a simpler alternative, $ABCD$ parameters can be used for the calculation of the normalized scattering parameters.

Figure 3 shows a two-port network terminated in arbitrary complex impedances Z_r and Z_L where $a_1, a_2, b_1,$ and b_2 are incident and reflected power waves and $V_1, V_2, I_1,$ and I_2 are voltages and currents at each port. Referring to (2.31) in [4] and (1) in [29], $a_1, a_2, b_1,$ and b_2 are expressed as

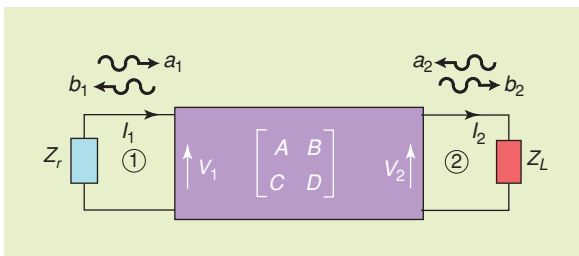


Figure 3. A two-port network with ABCD parameters.

$$a_1 = \frac{(V_1 + Z_r I_1)}{2\sqrt{\text{Re}(Z_r)}}, \quad b_1 = \frac{(V_1 - Z_r^* I_1)}{2\sqrt{\text{Re}(Z_r)}} \quad (10a)$$

$$a_2 = \frac{(V_2 + Z_L I_2)}{2\sqrt{\text{Re}(Z_L)}}, \quad b_2 = \frac{(V_2 + Z_L^* I_2)}{2\sqrt{\text{Re}(Z_L)}}. \quad (10b)$$

The input and output reflection coefficients are S_{11} and S_{22} and the transmission coefficient is $S_{12} = S_{21}$. The reflection and transmission scattering parameters are expressed in terms of $ABCD$ parameters as

$$S_{11} = \frac{b_1}{a_1} = \frac{V_1 - Z_r^* I_1}{V_1 + Z_r I_1} = \frac{AZ_L + B - CZ_r^* Z_L - DZ_r^*}{AZ_L + B + CZ_r Z_L + DZ_r}, \quad (11a)$$

$$S_{22} = \frac{b_2}{a_2} = \frac{V_2 + Z_L^* I_2}{V_2 + Z_L I_2} = \frac{-AZ_L^* + B - CZ_r Z_L^* + DZ_r}{AZ_L + B + CZ_r Z_L + DZ_r}, \quad (11b)$$

$$S_{21} = \frac{b_2}{a_1} = \frac{2\sqrt{\text{Re}(Z_r)}\sqrt{\text{Re}(Z_L)}}{AZ_L + B + CZ_r Z_L + DZ_r}. \quad (11c)$$

Symmetric Four-Port Networks

To derive design equations of the impedance-transforming directional couplers, the even- and odd-mode equivalent circuits are needed. The even- and odd-mode excitation analyses were first introduced by J. Reed and G. J. Wheeler [30] and have been used in various symmetrical three- and four-port power dividers such as Wilkinson power dividers, ring hybrids, branch-line hybrids, directional couplers, and so on.

A four-port network, being symmetric with respect to a symmetric line $S - S'$, is depicted in Figure 4(a) where a voltage source V_g is fed into port ①. If two signals of amplitude $V_g/2$ and in phase (even-mode excitation) are applied at ports ① and ② as shown in Figure 4(b), by symmetry a voltage maximum occurs at every point on the symmetry plane. That is, these points are all $Z = \bullet$ and $Y = \bullet$. This is equivalent to an open circuit, as illustrated in Figure 4(b). Similarly, if two signals of amplitude $V_g/2$ and 180° out of phase (odd-mode excitation) are applied at ports ① and ② as shown in Figure 4(c), a voltage minimum occurs at every point on the plane of symmetry. That is, these points are all $Z = \bullet$ and $Y = \bullet$. This is equivalent to a short circuit, as indicated in Figure 4(c). In each case, the problem is reduced to that of two-port equivalent networks. For the even-mode excitation, a reflection coefficient Γ_e and a transmission coefficient T_e are determined at port ①. Similarly, for the odd-mode excitation, a reflection Γ_o and a transmission coefficient T_o are also determined at port ①. By superposition, the

sum of the two cases is a signal V_g amplitude at port ①. The resulting signals out of the four ports are a superposition of those obtained from the even- and odd-mode excitations.

Thus, the vector amplitudes of the signals emerging from the four ports are

$$S_{11} = \frac{1}{2}(\Gamma_e + \Gamma_o), \quad (12a)$$

$$S_{21} = \frac{1}{2}(\Gamma_e - \Gamma_o), \quad (12b)$$

$$S_{31} = \frac{1}{2}(T_e - T_o), \quad (12c)$$

$$S_{41} = \frac{1}{2}(T_e + T_o). \quad (12d)$$

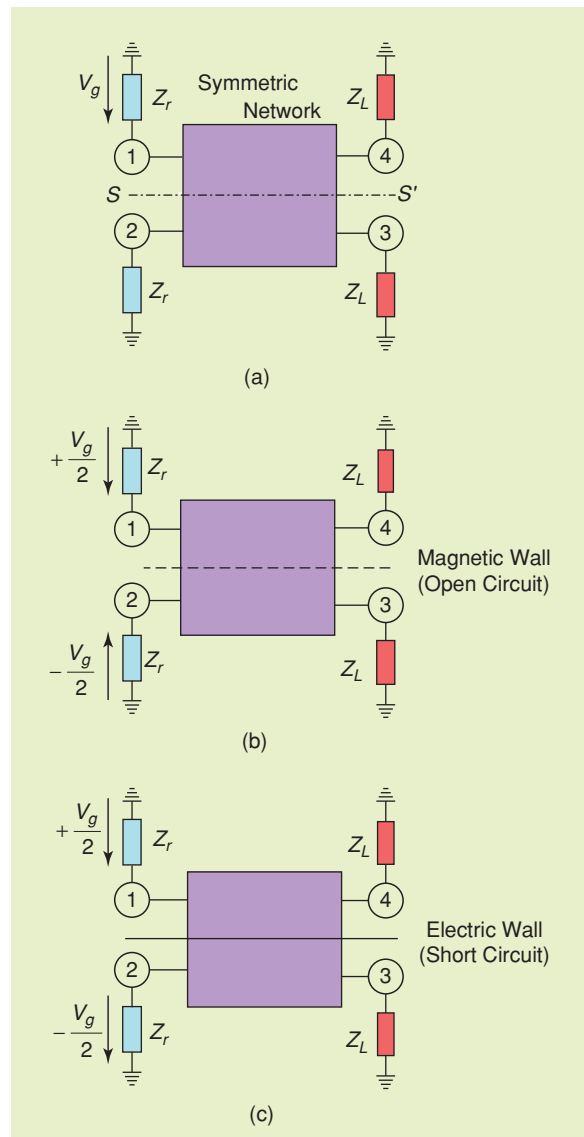


Figure 4. Symmetric four-port network. (a) Symmetric four-port network. (b) Even-mode excitation. (c) Odd-mode excitation.

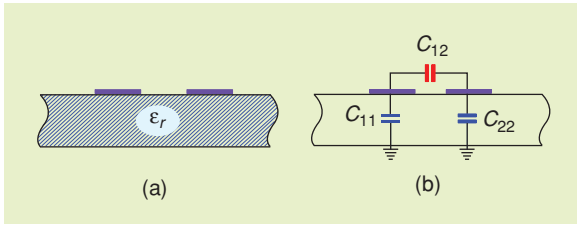


Figure 5. Coupled-transmission lines. (a) Coupled-transmission lines. (b) Equivalent capacitance network.

Impedance-Transforming Directional Couplers

Symmetric coupled transmission lines are shown in Figure 5 where coupled transmission lines are in Figure 5(a) and the equivalent capacitance network is shown in Figure 5(b). If a TEM (transverse electromagnetic) propagation of the two coupled transmission lines is assumed, then the characteristics of the coupled lines can be completely determined from the capacitances and the propagation velocity on the lines. In the equivalent capacitance network in Figure 5(b), C_{12} represents the capacitance between the two conductor lines in the absence of the ground conductor, while C_{11} and C_{22} denote the capacitances between each conductor and ground, in the absence of the other conductor line. If the coupled transmission lines are identical in size, then $C_{11} = C_{22}$.

For the even-mode excitation, no current flows between the two transmission lines, which leads to

$C_{12} = 0$. The resulting capacitance of either line to ground is $C_e = C_{11} = C_{22}$ and its characteristic impedance for the even-mode excitation, Z_{0e} is

$$Z_{0e} = \frac{1}{vC_e}, \quad (13)$$

where v is a propagation velocity on the line.

For the odd-mode excitation, the electric field lines have an odd symmetry about the center line and a voltage null exists between the two transmission lines, which leads to the effective capacitance between either conductor and ground $C_o = C_{11} + 2C_{12}$. Its characteristic impedance for the odd-mode excitation is

$$Z_{0o} = \frac{1}{vC_o}. \quad (14)$$

For the impedance-transforming directional couplers with Z_r and Z_L in Figure 1(a), the even- and odd-mode equivalent circuits are depicted as those in Figure 6. For the analyses, the (normalized) scattering parameters of the even- and odd-mode equivalent circuits need to be known. The reflection and transmission scattering parameters $\Gamma_{e,o}$ and $T_{e,o}$ can be calculated from either impedance, admittance, or $ABCD$ parameters, but the simplest way is from the $ABCD$ parameters.

How to Derive Equations (15) and (17)

The $ABCD$ parameters of the two equivalent circuits in Figure 6 are

$$\begin{bmatrix} A & B \\ C & D \end{bmatrix}_e = \begin{bmatrix} \cos \Theta & jZ_{0e} \sin \Theta \\ j\frac{\sin \Theta}{Z_{0e}} & \cos \Theta \end{bmatrix}, \quad (A1-a)$$

$$\begin{bmatrix} A & B \\ C & D \end{bmatrix}_o = \begin{bmatrix} \cos \Theta & jZ_{0o} \sin \Theta \\ j\frac{\sin \Theta}{Z_{0o}} & \cos \Theta \end{bmatrix}, \quad (A1-b)$$

where the even- and odd-mode electrical lengths are assumed to be the same for simplicity.

Substituting the even- and odd-mode $ABCD$ parameters into (11a) and (11c) gives

$$\Gamma_e = \frac{(Z_L - Z_r) \cos \Theta + j \left(Z_{0e} - \frac{1}{Z_{0e}} Z_L Z_r \right) \sin \Theta}{(Z_L + Z_r) \cos \Theta + j \left(Z_{0e} + \frac{1}{Z_{0e}} Z_L Z_r \right) \sin \Theta}, \quad (A2-a)$$

$$\Gamma_o = \frac{(Z_L - Z_r) \cos \Theta + j \left(Z_{0o} - \frac{1}{Z_{0o}} Z_L Z_r \right) \sin \Theta}{(Z_L + Z_r) \cos \Theta + j \left(Z_{0o} + \frac{1}{Z_{0o}} Z_L Z_r \right) \sin \Theta}, \quad (A2-b)$$

$$T_e = \frac{2}{\left(\sqrt{\frac{Z_L}{Z_r}} + \sqrt{\frac{Z_r}{Z_L}} \right) \cos \Theta + j \left(\frac{Z_{0e}}{\sqrt{Z_L Z_r}} + \frac{1}{Z_{0e}} \sqrt{Z_L Z_r} \right) \sin \Theta}, \quad (A2-c)$$

If the termination impedances Z_r and Z_L are assumed to be real, with reference to (11) and (12), S_{11} is computed as

$$S_{11} = \frac{1}{2}(\Gamma_e + \Gamma_o) = \frac{\text{Re}(N) + j \text{Im}(N)}{D}, \quad (15a)$$

where

$$\begin{aligned} \text{Re}(N) &= (Z_L^2 - Z_r^2) \cos^2 \Theta \\ &\quad - \left[\left(Z_{0e} Z_{0o} - \frac{1}{Z_{0e} Z_{0o}} (Z_L Z_r)^2 \right) \right] \sin^2 \Theta, \end{aligned} \quad (15b)$$

$$\text{Im}(N) = \left[(Z_{0e} + Z_{0o}) Z_L - Z_L Z_r \left(\frac{1}{Z_{0e}} + \frac{1}{Z_{0o}} \right) Z_r \right] \times \cos \Theta \sin \Theta, \quad (15c)$$

and D is a product of denominators of the even- and odd-mode reflection coefficients at port ①. (Also see “How to Derive Equations (15) and (17)”.)

For a matched directional coupler at ① in Figure 1(a), both $\text{Re}(N)$ and $\text{Im}(N)$ in (15) should be zero. In (15b), $\cos \Theta$ and $\sin \Theta$ cannot be zero at the same time and the termination impedances Z_L and Z_r are, in principle, different. Thus, the condition for the matched directional coupler is

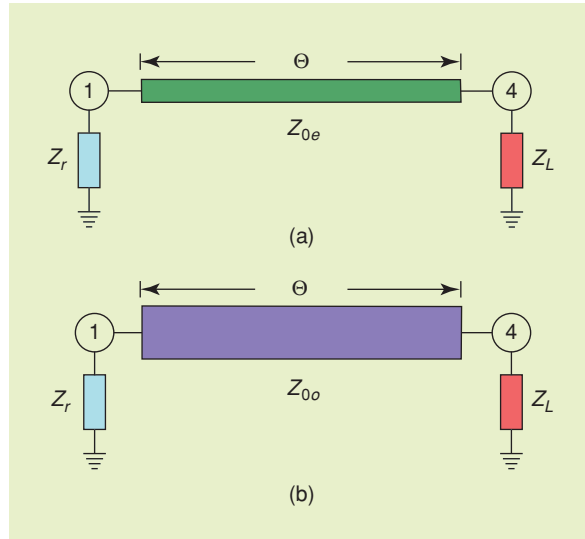


Figure 6. Even- and odd-mode equivalent circuits of the directional coupler symmetrically terminated in arbitrary impedances.

$$\Theta = 90^\circ \quad (16a)$$

$$Z_{0e} Z_{0o} = Z_L Z_r. \quad (16b)$$

For a fixed design frequency, the length of Θ is 90° but the electrical length is dependent on the operating

$$T_o = \frac{2}{\left(\sqrt{\frac{Z_L}{Z_r}} + \sqrt{\frac{Z_r}{Z_L}} \right) \cos \Theta + j \left(\frac{Z_{0o}}{\sqrt{Z_L Z_r}} + \frac{1}{Z_{0o}} \sqrt{Z_L Z_r} \right) \sin \Theta}, \quad (A2-d)$$

where the subscripts **e** and **o** denote the even- and odd-mode excitations. Thus, the scattering parameter of S_{11} is computed as (15).

Substituting a matching condition of $Z_{0e} Z_{0o} = Z_L Z_r$ into (A2) results in

$$\Gamma_e = \frac{(Z_L - Z_r) \cos \Theta + j(Z_{0e} - Z_{0o}) \sin \Theta}{(Z_L + Z_r) \cos \Theta + j(Z_{0e} + Z_{0o}) \sin \Theta}, \quad (A3-a)$$

$$\Gamma_o = \frac{(Z_L - Z_r) \cos \Theta - j(Z_{0e} - Z_{0o}) \sin \Theta}{(Z_L + Z_r) \cos \Theta + j(Z_{0e} + Z_{0o}) \sin \Theta}, \quad (A3-b)$$

$$T_e = T_o = \frac{2}{\left(\sqrt{\frac{Z_L}{Z_r}} + \sqrt{\frac{Z_r}{Z_L}} \right) \cos \Theta + j \left(\sqrt{\frac{Z_{0e}}{Z_{0o}}} + \sqrt{\frac{Z_{0o}}{Z_{0e}}} \right) \sin \Theta} \quad (A3-c)$$

It is noted that the even- and odd-mode reflection coefficients are same in magnitude but 180° out of phase, while the even- and odd-mode transmission scattering parameters are the same with each other. Using (12), the scattering parameters contributed by port ① are derived as those in (17).

frequencies. Therefore, for an arbitrary length of Θ , scattering parameters are obtained as

$$S_{11} = \frac{(Z_L - Z_r) \cos \Theta}{(Z_L + Z_r) \cos \Theta + j(Z_{0e} + Z_{0o}) \sin \Theta}, \quad (17a)$$

$$S_{21} = \frac{j(Z_{0e} + Z_{0o}) \sin \Theta}{(Z_L + Z_r) \cos \Theta + j(Z_{0e} + Z_{0o}) \sin \Theta}, \quad (17b)$$

$$S_{31} = 0, \quad (17c)$$

$$S_{41} = \frac{2}{\left(\sqrt{\frac{Z_L}{Z_r}} + \sqrt{\frac{Z_r}{Z_L}}\right) \cos \Theta + j\left(\sqrt{\frac{Z_{0e}}{Z_{0o}}} + \sqrt{\frac{Z_{0o}}{Z_{0e}}}\right) \sin \Theta}. \quad (17d)$$

(Also see “How to Derive Equations (15) and (17)”.)

When $\Theta = 90^\circ$, the scattering parameters are

$$S_{11} = 0, \quad (18a)$$

$$S_{21} = \frac{Z_{0e} - Z_{0o}}{Z_{0e} + Z_{0o}} = C, \quad (18b)$$

$$S_{31} = 0, \quad (18c)$$

$$S_{41} = -\frac{j2\sqrt{Z_{0e}Z_{0o}}}{Z_{0o} + Z_{0e}} = -j\sqrt{1 - C^2}, \quad (18d)$$

which prove that the power excited at port ① is delivered to ports ② and ④, and no power appears at port ③ in Figure 1(a). Using the passive properties (unitary and reciprocity properties), the scattering parameters characterizing the directional coupler with $\Theta = 90^\circ$ are

How to Derive Equation (21)

- Impedance transformation $IR = Z_r/Z_L$ is first defined.
- $|S_{11}|^2 = \frac{(Z_L - Z_r)^2 \sin^2 \Theta}{(Z_L + Z_r)^2 \cos^2 \Theta + (Z_{0e} + Z_{0o})^2 \sin^2 \Theta}$ is calculated from (17a).
- If the length of Θ is $\pi/2$ (90°) at a design center frequency f_0 , then it varies with an operating frequency f . So, Θ is substituted with $\pi/2 \cdot f/f_0$.
- To express $|S_{11}|^2$ containing the coupling coefficient of C , $(Z_{0e} + Z_{0o})^2 = (4Z_L Z_r)/(1 - C^2)$ is calculated using (20) and substituted.
- To express $|S_{11}|^2$ as a function of IR , divide both denominator and nominator by Z_L . Then the form of $|S_{11}|^2$ is obtained and the others are derived in a similar way.

$$[S] = \begin{bmatrix} 0 & C & 0 & -j\sqrt{1 - C^2} \\ C & 0 & -j\sqrt{1 - C^2} & 0 \\ 0 & -j\sqrt{1 - C^2} & 0 & C \\ -j\sqrt{1 - C^2} & 0 & C & 0 \end{bmatrix}. \quad (19)$$

With real termination impedances Z_L , Z_r and the coupling coefficient C specified, the required even- and odd-mode impedances are given as

$$Z_{0e} = \sqrt{\frac{(1 + C)}{(1 - C)}} Z_L Z_r, \quad (20a)$$

$$Z_{0o} = \sqrt{\frac{(1 - C)}{(1 + C)}} Z_L Z_r, \quad (20b)$$

which are design equations of the impedance-transforming directional couplers. If $Z_L = Z_r = Z_0$ in (20), they are well known design equations of directional couplers terminated in equal impedances, Z_0 [6], [9], [19], [31]–[33].

When $\Theta = \pi/2$ at a center frequency f_0 and unity power is fed into port ① in Figure 1(a), the powers appearing at each port are obtained as

$$|S_{11}|^2 = \frac{(1 - IR)^2 \cos^2\left(\frac{\pi}{2} \frac{f}{f_0}\right)}{(1 + IR)^2 \cos^2\left(\frac{\pi}{2} \frac{f}{f_0}\right) + 4IR \left(\frac{1}{1 - C^2}\right) \sin^2\left(\frac{\pi}{2} \frac{f}{f_0}\right)}, \quad (21a)$$

$$|S_{21}|^2 = \frac{4C^2 IR \sin^2\left(\frac{\pi}{2} \frac{f}{f_0}\right)}{(1 + IR)^2 (1 - C)^2 \cos^2\left(\frac{\pi}{2} \frac{f}{f_0}\right) + 4IR \sin^2\left(\frac{\pi}{2} \frac{f}{f_0}\right)}, \quad (21b)$$

$$|S_{31}|^2 = 0, \quad (21c)$$

$$|S_{41}|^2 = \frac{4}{\left(\sqrt{IR} + \frac{1}{\sqrt{IR}}\right)^2 \cos^2\left(\frac{\pi}{2} \frac{f}{f_0}\right) + \frac{4}{1 - C^2} \sin^2\left(\frac{\pi}{2} \frac{f}{f_0}\right)}, \quad (21d)$$

where $IR = Z_r/Z_L$, and C and f are coupling coefficient and operating frequency, respectively. (Also see “How to Derive Equation (21)”.) Based on the derived equations in (21), two types of calculations have been carried out using a mathematical program (Matlab 6). The first type is fixing a coupling coefficient at -3 dB and varying the impedance transformation ratio IR . The second is fixing an impedance transformation ratio IR at 1.5 and varying the coupling coefficients. The first and second types of calculation results are plotted in Figure 7 and Figure 8, respectively, where operating frequencies are normalized to a center frequency f_0 .

Matching performances are in Figure 7(a) and Figure 8(a), coupling powers in Figure 7(b) and Figure 8(b) and through powers ($|S_{41}|^2$) in Figure 7(c) and Figure 8(c). Figure 7(a) shows that a practical bandwidth decreases as the impedance transformation ratios increase. On the other hand, the bandwidth in Figure 8(a) is constant regardless of the coupling coefficients, when the impedance transformation ratio is fixed. In any case, perfect matching appears at the design center frequency, independently of the coupling coefficients and the impedance transformation ratios.

The three different scattering matrices are the same in the case of equal termination impedances but only the normalized scattering matrix is correct in the case of arbitrary termination impedances.

When the coupling coefficient is fixed, the coupling power is almost constant around a center frequency,

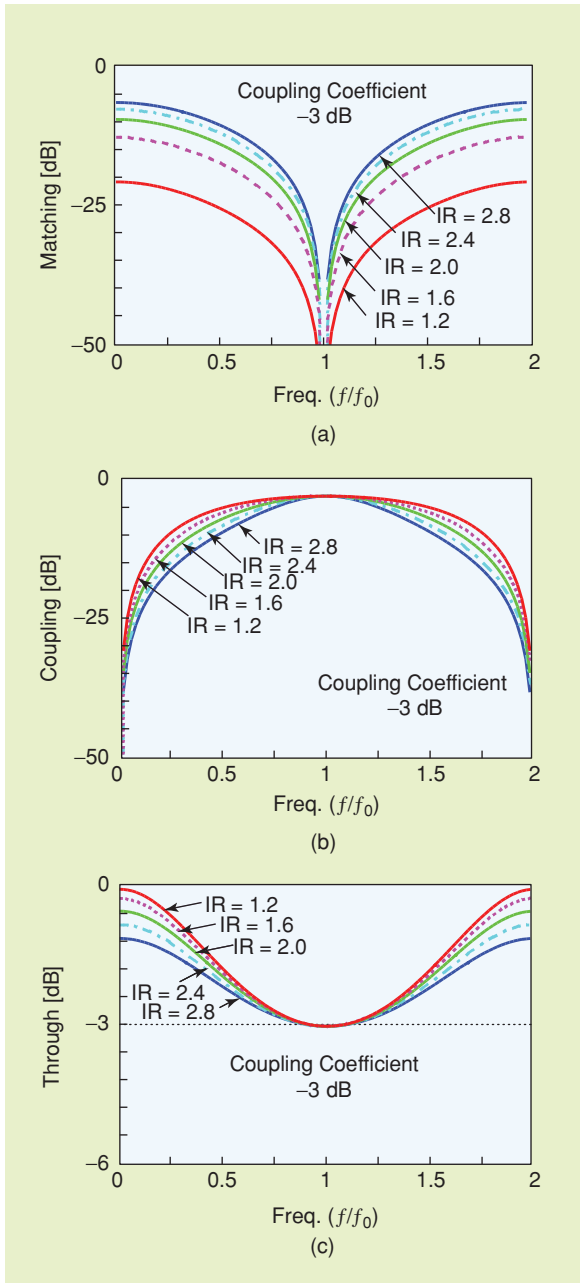


Figure 7. Calculation results with a fixed coupling coefficient of -3 dB and different impedance ratios: (a) matching, (b) coupling, and (c) through.

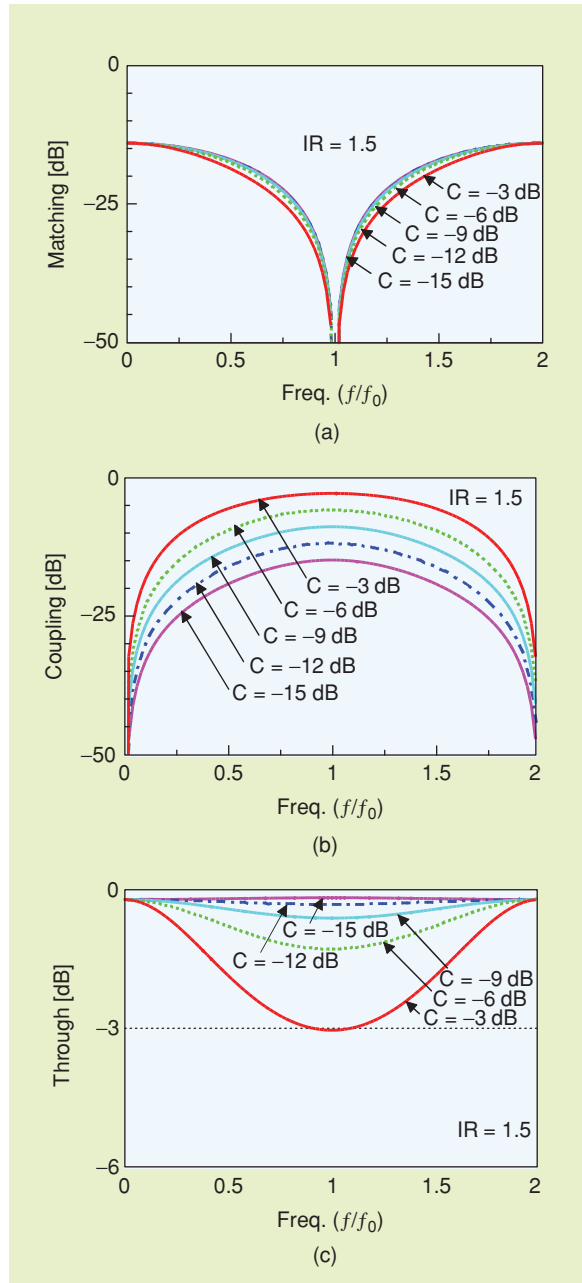


Figure 8. Calculation results with a fixed impedance transformation ratio $IR = 1.5$ and different coupling coefficients: (a) matching, (b) coupling, and (c) through.

If one can have any choice of the termination impedances of the directional couplers as shown in this article, the total size of a microwave integrated circuit can be reduced.

$$L = \frac{1}{|S_{41}|^2} = \frac{1}{|T_e|^2}, \quad (22)$$

and a positive quantity that is always greater than or equal to unity. In terms of $ABCD$ parameters, the power loss ratio L of the impedance transforming directional coupler with real termination impedances Z_r and Z_L is given as

$$L = 1 + \frac{1}{4} \left[\left(\sqrt{\frac{Z_L}{Z_r}} A_e - \sqrt{\frac{Z_r}{Z_L}} D_e \right)^2 - \left(\frac{B_e}{\sqrt{Z_L Z_r}} - C_e \sqrt{Z_L Z_r} \right)^2 \right]. \quad (23)$$

In the case of equal termination impedances $Z_L = Z_r = Z_0$, the power loss ratio [9] is given as

$$L_0 = 1 + \frac{1}{4} \left[(A_{e0} - D_{e0})^2 - \left(\frac{B_{e0}}{Z_0} - C_{e0} Z_0 \right)^2 \right]. \quad (24)$$

Comparing the two power loss ratios in (23) and (24), the following relation is obtained:

$$A_{e0} \rightarrow A_e \sqrt{\frac{Z_L}{Z_r}}, \quad (25a)$$

$$\frac{B_{e0}}{Z_0} \rightarrow \frac{B_e}{\sqrt{Z_L Z_r}}, \quad (25b)$$

$$C_{e0} Z_0 \rightarrow C_e \sqrt{Z_L Z_r}, \quad (25c)$$

$$D_{e0} \rightarrow D_e \sqrt{\frac{Z_r}{Z_L}}, \quad (25d)$$

where A_e , B_e , C_e , and D_e are even-mode $ABCD$ parameters with arbitrary termination impedances, and A_{e0} , B_{e0} , C_{e0} and D_{e0} are those with equal termination impedances.

Measurements

Based on the design equations in (20), a microstrip directional coupler with $Z_L = 50 \Omega$ and $Z_r = 30 \Omega$ was designed at a center frequency of 2 GHz, fabricated on a substrate ($\epsilon_r = 3.5$, $H = 30 \text{ mil}$, $\tan \delta = 0.04$), and measured. To adjust a coupling gap to 0.5 mm, the coupling coefficient was set to -16.6 dB . The corresponding Z_{0e} and Z_{0o} were 44.95Ω and 33.3Ω , respectively. Instead of the electrical length Θ , an average value of the even- and odd-mode electrical lengths was used [34]. Figure 9(a) shows the fabricated directional coupler where a dotted rectangle indicates the directional coupler and two impedance transformers are shown for the 30Ω termination

independently of the impedance transformation ratios as shown in Figure 7(b), while the coupling powers are directly dependent on the coupling coefficients with a fixed impedance transformation ratio of $IR = 1.5$ as shown in Figure 8(b). The through power is defined as $1 - C^2$ and dependent on the coupling coefficients as shown in Figure 8(c) but independent of the impedance transformation ratios as shown in Figure 7(c). From the calculation results in Figure 7 and Figure 8, we can conclude that the matching performances are dependent on only the impedance transformation ratios.

Power Loss Ratio

The power loss ratio L of a directional coupler is defined as

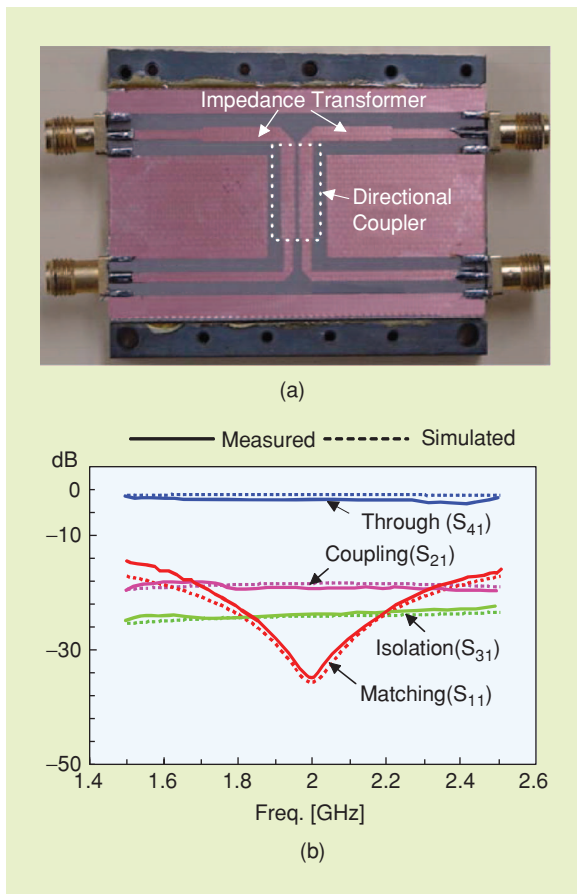


Figure 9. A microstrip directional coupler from [20]. (a) A fabricated directional coupler. (b) Results measured and simulated are compared.

impedances. Measured results are compared with simulated ones in Figure 9(b) where solid and dotted lines indicate measured and simulated results, respectively. The simulated matching, through, coupling, and isolation powers at 2 GHz are -34.7 dB, -0.63 dB, -17.1 dB, and -23 dB, respectively, and show good agreement with the measured ones.

Conclusions

Voltage-basis, current-basis, and normalized scattering matrices were introduced and it was shown that three different scattering matrices are the same only with equal termination impedances but only the normalized scattering matrix is correct with arbitrary termination impedances. The scattering matrices can be calculated from impedance, admittance, or *ABCD* matrices characterizing a network. However, if the network has more than three ports, the calculation process from the admittance or impedance matrices is not simple. For this, conversion formulas of the *ABCD* parameters into the normalized scattering parameters were presented for the impedance-transforming directional couplers. The directional couplers have been used and studied for more than 80 years, but all the theories and developments have been limited to equal termination impedances. Therefore, if one can have any choice of the termination impedances of the directional couplers as shown in this article, the total size of a microwave integrated circuit can be reduced.

References

- [1] G.A. Campbell and R.M. Foster, "Maximum output networks for telephone substation and repeater circuits," *Trans. AIEE*, vol. 39, pp. 1046–1054, 1920.
- [2] H.J. Calin, "The scattering matrix in network theory," *IRE Trans. Circuit Theory*, vol. CT-3, pp. 88–97, June 1956.
- [3] R.A. Rohrer, "The scattering matrix: Normalized to complex *n*-port load networks," *IEEE Trans. Circuit Theory*, vol. 12, pp. 223–230, June 1965.
- [4] H.-R. Ahn, *Asymmetric Passive Components in Microwave Integrated Circuits*. New York, Wiley, 2006, Ch. 2.
- [5] S.B. Cohn and R. Levy, "History of microwave passive components with particular attention to directional couplers," *IEEE Trans. Microwave Theory Tech.*, vol. MTT-32, pp. 1046–1054, Sept. 1984.
- [6] E.M.T. Hones and J.T. Bolljahn, "Coupled-strip-transmission-line filters and directional couplers," *IRE Trans. Microwave Theory Tech.*, vol. MTT-4, pp. 75–81, Apr. 1956.
- [7] S.B. Cohn, "Parallel-coupled transmission line resonators," *IRE Trans. Microwave Theory Tech.*, vol. MTT-6, pp. 223–231, Apr. 1958.
- [8] G.L. Matthaei, "Interdigital bandpass filters," *IRE Trans. Microwave Theory Tech.*, vol. MTT-10, pp. 479–491, Nov. 1962.
- [9] R. Levy, "General synthesis of asymmetric multi-element coupled transmission line directional couplers," *IEEE Trans. Microwave Theory Tech.*, vol. MTT-11, pp. 227–231, July 1963.
- [10] E.G. Cristal, "Coupled-transmission-line directional couplers with coupled lines of unequal characteristic impedances," *IEEE Trans. Microwave Theory Tech.*, vol. MTT-14, pp. 337–346, July 1966.
- [11] J.P. Shelton, "Impedances of offset parallel-coupled strip transmission lines," *IEEE Trans. Microwave Theory Tech.*, vol. MTT-14, pp. 7–15, May 1966.
- [12] J.P. Shelton and J.A. Mosko, "Synthesis and design of wideband equal ripple TEM directional couplers and fixed phase shifters," *IEEE Trans. Microwave Theory Tech.*, vol. MTT-14, pp. 462–473, Oct. 1966.
- [13] C.B. Sharpe, "An equivalence principle for nonuniform transmission-line directional couplers," *IEEE Trans. Microwave Theory Tech.*, vol. MTT-15, pp. 398–405, July 1967.
- [14] G.I. Zysman and A.K. Johnson, "Coupled transmission line networks in an inhomogeneous dielectric medium," *IEEE Trans. Microwave Theory Tech.*, vol. MTT-17, pp. 753–759, Oct. 1969.
- [15] M.K. Krage and G.I. Haddad, "Characteristics of coupled microstrip transmission lines-I: Coupled-mode formulation of inhomogeneous lines," *IEEE Trans. Microwave Theory Tech.*, vol. MTT-18, pp. 217–222, Apr. 1970.
- [16] K.D. Marx, "Propagation modes equivalent circuits, and characteristic terminations for multiconductor transmission lines with inhomogeneous dielectrics," *IEEE Trans. Microwave Theory Tech.*, vol. MTT-21, pp. 450–457, July 1973.
- [17] U.H. Gysel, "New theory and design for hairpin-line filters," *IEEE Trans. Microwave Theory Tech.*, vol. MTT-22, pp. 523–531, May 1974.
- [18] V.J. Tripathi, "Asymmetric coupled transmission lines in an inhomogeneous medium," *IEEE Trans. Microwave Theory Tech.*, vol. MTT-23, pp. 734–739, Sept. 1975.
- [19] D.F. Williams, L.A. Hayden and R.B. Marks, "A complete multi-mode equivalent-circuit theory for electrical design," *NIST J. Res.*, vol. 102, no. 4, pp. 405–423, July–Aug., 1997.
- [20] H.-R. Ahn and B. Kim, "Transmission-line directional couplers for impedance transforming," *IEEE Microwave Wireless Components Lett.*, vol. 16, no. 10, pp. 537–539, Oct. 2006.
- [21] H.-R. Ahn, I.-S. Chang, and S.-W. Yun, "Miniaturized 3-dB ring hybrid terminated by arbitrary impedances," *IEEE Trans. Microwave Theory Tech.*, vol. 42, pp. 2216–2221, Dec. 1994.
- [22] H.-R. Ahn, I. Wolff, and I.-S. Chang, "Arbitrary termination impedances, arbitrary power division and small-sized ring hybrids," *IEEE Trans. Microwave Theory Tech.*, vol. 44, pp. 2241–2247, Dec. 1997.
- [23] H.-R. Ahn and I. Wolff, "Asymmetric four-port and branch-line hybrids," *IEEE Trans. Microwave Theory Tech.*, vol. 48, pp. 1585–1588, Sept. 2000.
- [24] H.-R. Ahn and I. Wolff, "Three-port 3-dB power divider terminated by different impedances and its application to MMIC's," *IEEE Trans. Microwave Theory Tech.*, vol. 47, pp. 786–794, June 1999.
- [25] H.-R. Ahn and I. Wolff, "General design equations of three-port power dividers, small-sized impedance transformers, and their applications to small-sized three-port 3-dB power dividers," *IEEE Trans. Microwave Theory Tech.*, vol. 49, pp. 1277–1288, July 2001.
- [26] H.-R. Ahn and I. Wolff, "Asymmetric ring hybrid phase shifters and attenuators," *IEEE Trans. Microwave Theory Tech.*, vol. 50, pp. 1146–1155, Apr. 2002.
- [27] Y. Yang, Y. Woo, and B. Kim, "Optimization for error-canceling loop of the feedforward amplifier using a new system-level mathematical model," *IEEE Trans. Microwave Theory Tech.*, vol. 51, pp. 475–482, Feb. 2003.
- [28] Y. Yun, Y. Yang, J. Yi, J. Nam, J. Cha, and B. Kim, "A new adaptive feedforward amplifier for WCDMA base stations using imperfect signal cancellation," *Microwave J.*, vol. 46, no. 4, pp. 22–44, Apr. 2003.
- [29] K. Kurokawa, "Power waves and the scattering matrix," *IEEE Trans. Microwave Theory Tech.*, vol. MTT-13, pp. 194–202, Mar. 1965.
- [30] J. Reed and G.J. Wheeler, "A method of analysis of symmetrical four-port networks," *IRE Trans. Microwave Theory Tech.*, vol. 4, pp. 346–352, Oct. 1956.
- [31] R. Mongia, I. Bahl, and P. Bhartia, *RF and Microwave Coupled-Line Circuits*, Boston, Artech House, 1999, pp. 183, 190, 366.
- [32] D.-M. Pozar, *Microwave Engineering*, New York: Addison-Wesley, 1990, p. 425.
- [33] G.-L. Matthaei, L. Young, and E.M.T. Jones, *Microwave Filters, Impedance-Matching Networks, and Coupling Structures*. New York: McGraw-Hill, 1980, p. 779.
- [34] D. Kajfez and B.S. Vidula, "Design equations for symmetric microstrip DC blocks," *IEEE Trans. Microwave Theory Tech.*, vol. MTT-28, no. 9, pp. 974–981, 1980. 